

XONOTLITE IN RODINGITE ASSEMBLAGES FROM THE RONDA PERIDOTITES, BETIC CORDILLERAS, SOUTHERN SPAIN

JOSÉ JULIÁN ESTEBAN[§], JULIA CUEVAS and JOSÉ M. TUBÍA

*Departamento de Geodinámica, Facultad de Ciencias,
Universidad del País Vasco, a.p. 644, E-48080 Bilbao, Spain*

IÑAKI YUSTA

*Departamento de Mineralogía y Petrología, Facultad de Ciencias,
Universidad del País Vasco, a.p. 644, E-48080 Bilbao, Spain*

ABSTRACT

Xonotlite, ideally $\text{Ca}_6\text{Si}_6\text{O}_{17}(\text{OH})_2$, occurs as a major phase in the leucocratic dyke complex that intruded the Ronda peridotites, near the village of Carratraca, Málaga, Spain. Xonotlite occurs as acicular grains in veins parallel to the dykes, as tabular grains along the reaction zone between the serpentinite host-rock and the leucocratic dykes, and as acicular grains replacing hydrogrossular in the matrix of the dykes. It is associated with albite, pectolite and hydrogrossular. Electron-microprobe analyses give a formula $(\text{Ca}_{6.05})(\text{Si}_{5.96}\text{Al}_{0.01})\text{O}_{17}(\text{OH})_2$ for the acicular and tabular xonotlite, and $(\text{Ca}_{6.11})(\text{Si}_{5.92}\text{Al}_{0.03})\text{O}_{17}(\text{OH})_2$ for xonotlite replacing hydrogrossular. X-ray powder-diffraction patterns of xonotlite show the presence of two polytypes: *M2a2b2c* and *Ma2b2c*. This unusual association (xonotlite, hydrogrossular, pectolite) was produced by the rodingitization of the leucocratic dykes during the serpentinitization of the ultramafic massif at low-temperature conditions, 300° to 350°C; it was associated with the production of lizardite in the surrounding serpentinites.

Keywords: xonotlite, hydrogrossular, polytypes, rodingite, rodingitization, chemical data, powder-diffraction data, Ronda peridotites, Betic Cordilleras, Málaga, Spain.

SOMMAIRE

La xonotlite, dont la composition idéale est $\text{Ca}_6\text{Si}_6\text{O}_{17}(\text{OH})_2$, constitue une phase majeure dans l'essai de filons leucocrates qui recoupe les péridotites du massif de Ronda, près du village de Carratraca, Málaga, en Espagne. La xonotlite se présente en grains aciculaires dans des veines parallèles aux filons, en grains tabulaires le long de la zone de réaction entre les serpentinites hôtes et les filons leucocrates, et en grains aciculaires en remplacement de l'hydrogrossulaire dans la matrice des filons. Elle montre une association avec albite, pectolite et hydrogrossulaire. Les analyses à la microsonde électronique ont mené à la formule $(\text{Ca}_{6.05})(\text{Si}_{5.96}\text{Al}_{0.01})\text{O}_{17}(\text{OH})_2$ pour la xonotlite aciculaire et tabulaire, et $(\text{Ca}_{6.11})(\text{Si}_{5.92}\text{Al}_{0.03})\text{O}_{17}(\text{OH})_2$ pour la xonotlite en remplacement de l'hydrogrossulaire. Les spectres de diffraction X (méthode des poudres) démontrent la présence de deux polytypes, *M2a2b2c* et *Ma2b2c*. Cette association inhabituelle (xonotlite, hydrogrossulaire, pectolite) résulte de la rodingitisation des filons leucocrates au cours de la serpentinitisation du massif ultramafique à faibles températures, entre 300° et 350°C; elle s'est formée en association avec la lizardite dans les roches encaissantes.

(Traduit par la Rédaction)

Mots-clés: xonotlite, hydrogrossulaire, polytypes, rodingite, rodingitisation, données chimiques, données de diffraction X, péridotites de Ronda, Cordillères Bétiques, Málaga, Espagne.

[§] E-mail address: gpbegu@lg.ehu.es

INTRODUCTION

Rodingites are produced from a variety of protoliths by the Ca-metasomatism associated with the serpentinization in nearby ultramafic rocks (O'Hanley 1996). The interest in rodingites within ophiolite sequences is twofold: 1) they are good markers of low-temperature alteration developed at shallow levels (Coulton *et al.* 1995), and 2) they can be preserved and recognized after high-pressure metamorphic events. For example, Puga *et al.* (1999) described relics of rodingite within eclogites in the Nevado-Filábride Complex of the Betic Cordilleras of southern Spain, and claimed they are evidence for the existence of an extensional oceanic setting prior to the involvement of the complex in the Alpine subduction event.

The aim of this contribution is to provide a description of rodingites reported for the first time in the Ronda peridotites, in the Betic Cordilleras, Spain, with a focus on the occurrence of xonotlite. The study of the rodingite is important in understanding the emplacement history of the Ronda peridotites, and hence the geodynamic models of the Betic Cordilleras. Previous works on the Ronda peridotites have only taken into account their high-temperature evolution (Tubía & Cuevas 1986, Van der Wal & Vissers 1996). Our data will help to constrain later, low-temperature stages in the emplacement history.

BACKGROUND INFORMATION

The occurrence of rodingites in peridotite massifs reflects the production of Ca-rich fluids during the serpentinization of peridotites. Such fluids are generated owing to the inability of the structure of serpentinite minerals to accept the calcium (Schandl *et al.* 1990) released from pyroxenes. These Ca-rich fluids react with other rocks in contact with the ultramafic rocks, which are transformed to assemblages of calcium silicates, including hydrogrossular, epidote, vesuvianite, diopside and pectolite. Xonotlite has been found only rarely in rodingites (Coleman 1967).

Xonotlite, a hydrous calcium silicate, ideally $\text{Ca}_6\text{Si}_6\text{O}_{17}(\text{OH})_2$, was first reported from the type locality at Tetela de Xonotla in Mexico by Rammelsberg in 1866 (in de Bruijn *et al.* 1999). It occurs in two main associations, in hornfels near limestone layers (Brown 1978) and associated with intrusive mafic bodies (Schwartz 1924, 1925, Shannon 1925, Bauer & Berman 1935, Kaye 1953, Smith 1954, Coombs & Lauder 1960, O'Brien & Rodgers 1973, Jakobsson & Moore 1986). Xonotlite can be formed experimentally by the decomposition of tobermorite (Taylor 1959, Buckner *et al.* 1960, Speakman 1968), by the dehydration of truscottite and gyrolite, or by the hydration of wollastonite (Roy 1958, Harker 1964).

In the samples studied, xonotlite mainly occurs in late veinlets associated with cordierite-bearing granitic

dykes that intrude in the Ronda peridotites. In thin section, xonotlite appears as 1×0.12 mm prisms and as tiny needles, only 0.07 mm long. Xonotlite is commonly associated with hydrogrossular, pectolite, chlorite, prehnite and albite. This association of minerals, typical of rodingitization processes (Coleman 1967), reveals that Ca-metasomatism affected the granitic dykes during the serpentinization of the Ronda peridotites.

GEOLOGICAL SETTING

The Ronda peridotites are the largest mass of orogenic lherzolite in the world. They form part of the Alpujárride Complex of the Internal Zone of the Betic Cordilleras (Figs. 1A, B). The Betic Cordilleras correspond to the westernmost segment of the peri-Mediterranean Alpine orogen. This belt was formed during the Africa-Iberia convergence from Late Cretaceous to Tertiary time (Dewey *et al.* 1989). The Alpujárride Complex encompasses a stack of allochthonous metamorphic tectonic units (Tubía *et al.* 1992). The Ronda peridotites are the lower portion of the highest Alpujárride thrust sheet (Navarro-Vilá & Tubía 1983, Tubía & Cuevas 1986).

The term Ronda peridotites is applied to a group of orogenic lherzolite masses (Sierra Bermeja, Sierra Alpujata, Carratraca, Mijas; Fig. 1B) forming slabs with a thickness of 1.5 to 2 km (Lundeen 1978, Tubía 1994). They are mainly composed of lherzolite, with subordinate amounts of harzburgite, dunite and mafic layers (Hernández Pacheco 1967). In the Sierra Bermeja (Obata 1980) and Sierra Alpujata massifs (Tubía 1994), there is a large-scale zonation from plagioclase peridotite below, spinel peridotite at intermediate levels, to garnet peridotite in the uppermost part of the ultramafic slabs. This reverse zonation reflects a pressure decrease down-section and points to a complex exhumation of the Ronda peridotites from mantle depths (Obata 1980). Several dykes of cordierite-bearing granite intrude the Ronda peridotites (Hernández Pacheco 1967, Dickey & Obata 1974). The dykes are less than 0.5 m in width, and show sharp contacts with the ultrabasic rocks.

Rodingites were collected from the granite dyke complex in the Carratraca Massif. The samples of xonotlite were taken (Fig. 2) from a prominent outcrop in a cut along the Málaga-Campillos road (A-357). From a structural point of view, this outcrop corresponds to a back-tilted extensional shear-zone, the Cerro Tajo Fault (Argles *et al.* 1999), which juxtaposes migmatites with serpentinized spinel peridotites. The road-cut exposes many granitic dykes injected in the ultrabasic rocks, along a system of joints parallel to the Cerro Tajo Fault (Fig. 3A). An unusual feature of the rodingites from the Carratraca massif, but fairly common along the Cerro Tajo section, is the presence of xonotlite veins. Figure 3B shows that these veins are parallel to the dyke's walls, and that they occur in the granite and in the serpentinite. The xonotlite veins, ranging in thick-

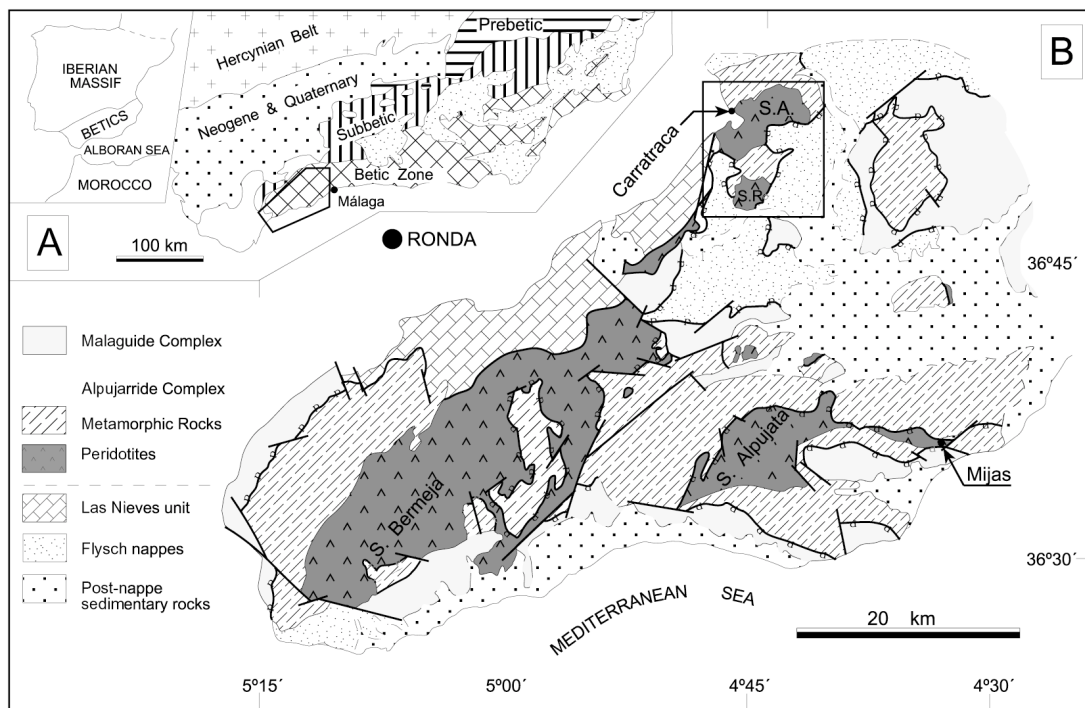


FIG. 1. A. Location of the study zone in the Betic Cordilleras, west of Málaga. B. Simplified geological map of the western sector of the Betic Cordilleras, showing the main complexes of the Ronda peridotites: Sierra Bermeja, Sierra Alpujata, Mijas and Carratraca (from Tubía 1994).

ness from 1 mm to 1.5 cm, are white in hand specimen (Fig. 4D), with a white streak and silky luster. The contacts between several dykes and the peridotites and some joints within the ultrabasic rocks are coated with films of randomly arranged crystals of aragonite. Tiny fibrous crystals of aragonite were also optically observed in microcracks that cross-cut xonotlite veins and the serpentinite fabric.

At the Cerro Tajo section, the primary assemblages of the dyke rocks include biotite, cordierite, zoned plagioclase ($An_{80}-An_{38}$), and quartz. Ilmenite, apatite and zircon are minor minerals. Garnet is also present locally, as inclusions in cordierite. Crystals of cordierite and plagioclase have euhedral to subhedral shapes. Some of the cordierite crystals have hourglass twins or epitactic microstructures outlined by small inclusions of biotite, sillimanite and quartz. Grain sizes range from very fine-grained to medium-grained, and the rocks may display either equigranular or porphyritic textures. In the thicker dykes, the biotite, cordierite and plagioclase display a common preferred orientation that defines a foliation parallel to the dyke contacts. Graphite occurs as small interstitial grains. Some samples, with up to 3% of graphite, are similar to the “ordered graphitic hornfels

dykes” observed in the Sierra Bermeja massif by Dickey & Obata (1974). According to Dickey & Obata (1974) and Luque *et al.* (1987, 1992), the source of graphite might have been sedimentary hydrocarbons trapped in muds that experienced anatexis during the high-temperature emplacement of the Ronda peridotites.

The rodingitized dykes at Cerro Tajo are white to light grey, with a porcellaneous look, and are commonly brecciated. These rodingite rocks are characterized by the lack of quartz and by the occurrence of albite, chlorite, hydrogrossular, prehnite and pectolite. Most of these fine-grained minerals display prismatic habits and form either radial aggregates or interpenetrating textures. Pectolite + albite veins were previously documented in a granitic dyke within the peridotites of the Sierra Bermeja massif by Dickey & Obata (1974). However, these authors did not relate such minerals to a rodingitization processes. The hydrogrossular and chlorite are concentrated in very thin selvages developed along the borders of the dykes. The hydrogrossular usually form clusters of rounded grains, less than 0.1 mm in diameter, armored in chlorite. Less commonly, the hydrogrossular is found within the groundmass of the rodingite, as large crystals partly replaced by xonotlite

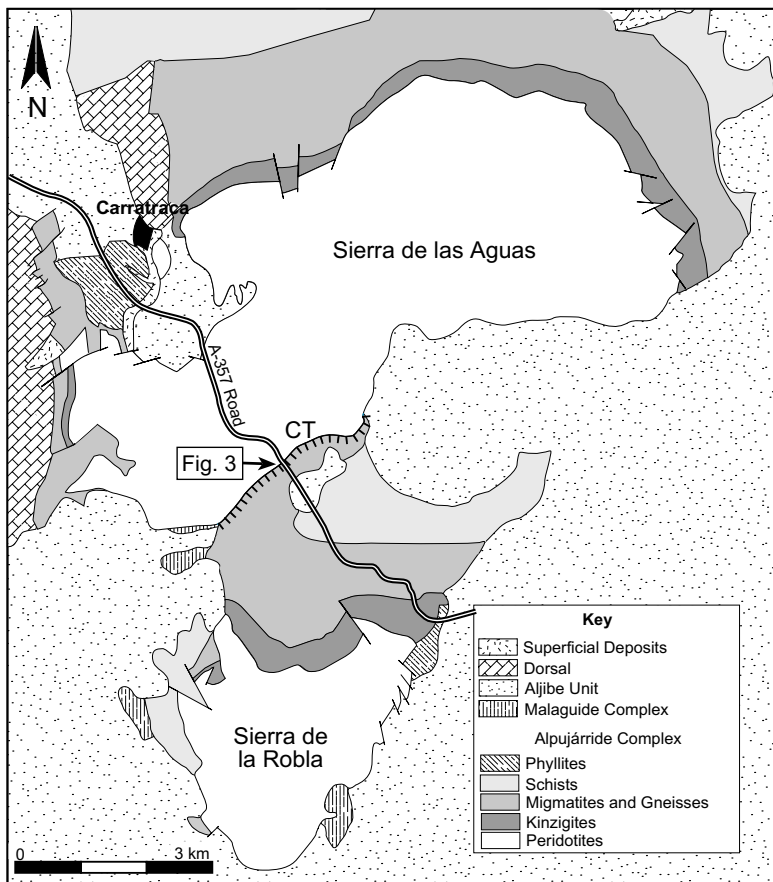


Fig. 2. Geological map of Carratraca area (see location on Figure 1B). The samples of xonotlite were collected along the A-357 road (Málaga-Campillos), as indicated in Figure 3. CT: Cerro Tajo extensional fault (modified after Argles *et al.* 1999).

(Fig. 4B). The pectolite crystals range in size from 0.1 to 1.0 mm, and occur as prismatic grains dispersed throughout the rodingitized dykes. In some dykes, the pectolite is concentrated in veins, more than 2 cm in width, at a high angle to the dyke walls. The monomineralic veins are composed of needle-shaped crystals, up to 0.5 cm long, forming radial aggregates. The pectolite-rich rodingitized dykes usually lack hydrogrossular. The surrounding serpentinites are mainly composed of lizardite with a mesh or hourglass texture and interstitial magnetite.

Xonotlite is also a major component of a few rodingitized dykes. Xonotlite occurs as acicular aggregates (Fig. 4A), isolated tabular grains (Fig. 4C) and acicular aggregates replacing hydrogrossular (Fig. 4B). Acicular aggregates are concentrated chiefly in veins up to 1 cm thick and are parallel to the dyke walls (Fig. 3B). These acicular aggregates display a strong pre-

ferred orientation at high angle to the veins (Fig. 4A). Density measurements for acicular aggregates of xonotlite by flotation in high-density liquids give values of 2.67 g/cm³. The small tabular grains are isolated in the matrix of the dykes or occur in the reaction zone between the serpentinite host and the granitic dykes.

CHEMICAL COMPOSITION

Quantitative chemical data of the xonotlite from the Ronda peridotites were determined by electron-microprobe analysis (EMPA) using a CAMEBAX SX-50 instrument with the following operating conditions: excitation voltage 15 kV, beam current 15 nA and counting time 10 s. Crystals were analyzed using BRGM standards and corrected by means of the ZAF method.

Single tabular ($n = 6$) and acicular ($n = 13$) grains from the veins, and xonotlite replacing hydrogrossular

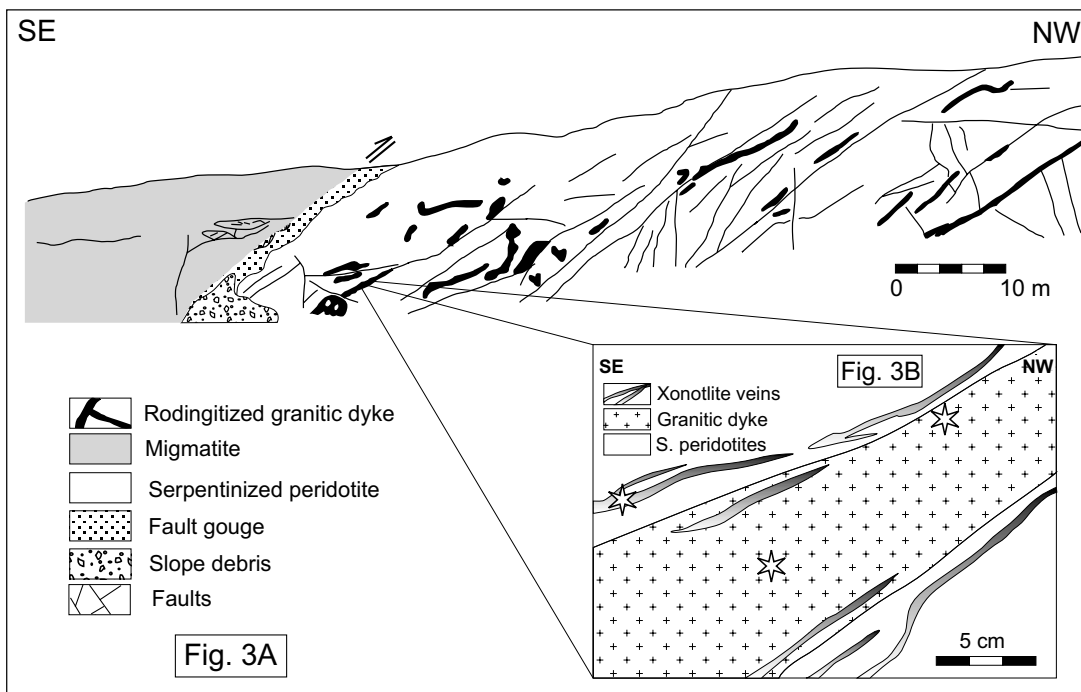


FIG. 3. A. Detailed cross-section of the Cerro Tajo fault. B. Schematic relations between xonotlite veins, serpentinized peridotites and rodingitized granitic dykes. Stars indicate the location of the samples studied.

TABLE 1. XONOTLITE FROM THE RONDA PERIDOTITES: AVERAGE COMPOSITION AND RANGE, AND STRUCTURAL FORMULAE

	Tabular and acicular		Acicular replacing Hgr	
	median <i>n</i> = 19*	range	median <i>n</i> = 16	range
SiO ₂ wt. %	50.07	48.61 - 50.77	49.32	46.30 - 50.27
TiO ₂	0.00	0.00 - 0.03	0.01	0.00 - 0.05
Al ₂ O ₃	0.04	0.00 - 0.48	0.20	0.01 - 0.54
Cr ₂ O ₃	0.02	0.00 - 0.13	0.02	0.00 - 0.11
FeO	0.07	0.00 - 0.49	0.02	0.00 - 0.56
MnO	0.03	0.00 - 0.32	0.04	0.00 - 0.43
MgO	0.00	0.00 - 0.53	0.00	0.00 - 0.63
CaO	47.39	44.28 - 48.77	47.56	44.96 - 48.99
Na ₂ O	0.02	0.00 - 0.10	0.02	0.00 - 0.06
K ₂ O	0.01	0.00 - 0.03	0.02	0.00 - 0.04
Structural formula, on the basis of 18 atoms of oxygen (excluding H ₂ O')				
Si <i>apfu</i>	5.96		5.92	
Al	0.01		0.03	
Ca	6.05		6.11	

Hgr: hydrogrossular. * (*n* = 6) + (*n* = 13).

(*n* = 16) were analyzed. Despite the textural differences in the xonotlite from veins, their chemical compositions are very similar, so the results are averaged in the same group (Table 1). Maximum FeO (0.56 wt.%), MgO, MnO and Al₂O₃ are found in parts of xonotlite grains associated with hydrogrossular, and possibly reflect garnet impurities. The average formula is (Ca_{6.05})(Si_{5.96}Al_{0.01})O₁₇(OH)₂ for the xonotlite veins and (Ca_{6.11})(Si_{5.92}Al_{0.03})O₁₇(OH)₂ for xonotlite needles associated with hydrogrossular.

The thermogravimetric analysis of xonotlite was done using a SDT2960 simultaneous DTA/TGA system (TA Instruments) coupled to a Mass Spectrometer Gas Analyzer (MS ThermoStar, Balzers Instruments) for on-line determination of N₂, C–O, CO₂, and H₂O. A hand-picked sample from a 1-cm-thick vein of xonotlite (~50 mg) was ground to a fine powder in a mixer mill (MM200, Retsch with zirconia grinding hardware), run in Pt crucible and heated at 5°C/min from room temperature up to 900°C; we monitored the weight and the evolved (reaction) gases with time. The sample atmosphere was He gas flowing at 60 mL/min.

Two weight-loss maxima were identified in the thermogram. The first loss at about 450° to 650°C probably

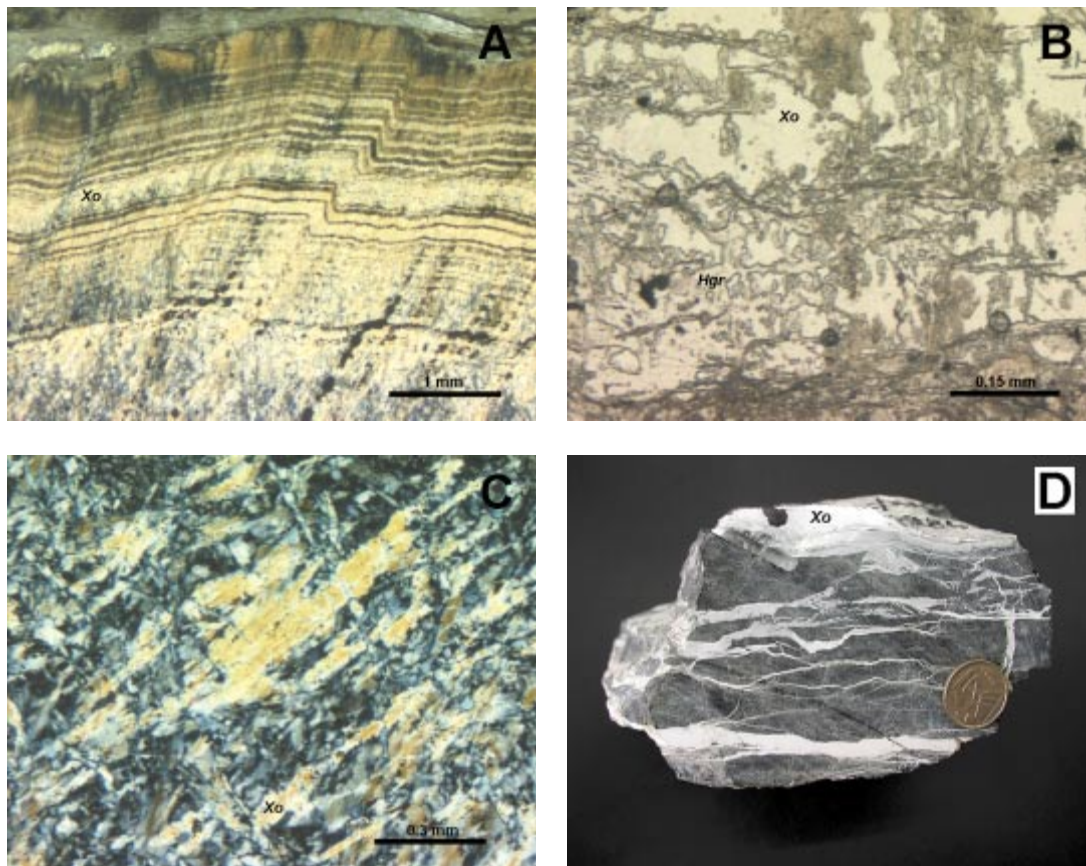


FIG. 4. Photomicrographs of xonotlite. A. Acicular xonotlite (Xo) in veins. B. Xonotlite (Xo) partially replacing hydrogrossular (Hgr). C. Tabular grains of xonotlite (Xo). D. Detailed view of white xonotlite veins (Xo) within serpentinized peridotites. Diameter of coin is 1.7 cm.

represents the breakdown of aragonite, as the corresponding gas analysis confirms that CO_2 was produced during heating. The yield, ~ 3.3 wt % of CO_2 , corresponds to about 7.5% aragonite. Aragonite has been also identified in the XRD analysis (using the most intense peaks at 3.397 and 1.977 Å in the PDF pattern 41-1475). The second weight-loss in the MS-curve occurs in the range of 740° to 820°C, and represents the loss of hydroxyl as H_2O from the xonotlite. After subtracting the mass of aragonite, a weight loss of about 2.3% is calculated for the 740°–820°C interval, accounting for 92% of the stoichiometric H_2O expected in xonotlite. In a previous determination of the H_2O content on natural specimens of xonotlite by TGA/DSC, Shaw *et al.* (2000) reported a weight loss of 2.5% for the 770°–880°C interval. The totals of the microprobe-derived chemical data have been lowered by ~ 2.4 wt% in accordance with the TGA data (Table 1).

X-RAY POWDER-DIFFRACTION DATA

Unfortunately, material suitable for single-crystal X-ray examination was not found, so that the identification of xonotlite was done on polycrystalline aggregates separated from xonotlite-rich veins. X-ray powder-diffraction (XRPD) data were obtained at the “Servicio de Análisis de Minerales y Rocas” of the Universidad del País Vasco. The diffraction pattern was recorded for 10 h with a Philips PW 1710 diffractometer and using a PW 1729 generator operating at the following conditions: 40 kV, beam current 20 mA, $\text{CuK}\alpha$ radiation (λ 1.5406 Å), graphite monochromator, step-scan in the 2θ region 10–70° in 0.025° 2θ steps.

The main diffraction-peaks of xonotlite in veins, compared to published and calculated XRD patterns of xonotlite, are shown in Table 2. The data are generally in good agreement with the spacings of the PDF 29-0379 diffraction pattern (ICDD Mineral Powder Dif-

TABLE 2. POWDER-DIFFRACTION DATA FOR XONOTLITE FROM THE RONDA PERIDOTITES, COMPARED WITH PUBLISHED PATTERNS

This work		JCPDS 29-0379		Xon- <i>M2a2b2c</i>		Xon- <i>Ma2b2c</i>		This work		JCPDS 29-0379		Xon- <i>M2a2b2c</i>		Xon- <i>Ma2b2c</i>		
<i>d</i> _{obs}	<i>I</i> ₀	<i>hkl</i>	<i>d</i>	<i>I</i> ₀	<i>hkl</i>	<i>d</i> _{calc}	<i>I</i> ₀	<i>hkl</i>	<i>d</i> _{calc}	<i>I</i> ₀	<i>hkl</i>	<i>d</i>	<i>I</i> ₀	<i>hkl</i>	<i>d</i> _{calc}	<i>I</i> ₀
8.527	2	2 0 0	8.520	7	1 0 0	8.516	12	$\bar{2}$ 0 0	8.516	8	12b	2.637	12	$\bar{6}$ 0 1	2.636	9
6.998	32	0 0 1	7.000	30	0 0 2	7.011	58	0 0 $\bar{2}$	7.011	31	2.637	2.613	3	6 0 1	2.617	5b
6.505	1	$\bar{1}$ 0 1	6.510	7b	0 1 1	6.519	8	0 1 1	6.519	8		2.596	2	0 1 5	2.612	8
6.499	6.418	<1	1 0 1	6.420	4b	0 $\bar{1}$ 1	6.406	8	0 1 1	6.400	22	2.505	20	1 2 2	2.507	20
						0 1 1	6.400	22						1 2 4	2.509	19
														5 2 0	2.498	10
														0 0 3	2.335	12
6.077	<1													1 0 6	2.257	25
5.641	<1													2 1 5	2.161	3
5.613	<1	3 0 0	5.620	1										2 1 5	2.148	1
5.430	1													4 0 0	2.129	2
														2 1 0 5	2.109	1
														2 0 4 0	2.040	40
														5 2 2	2.039	30
4.708	<1													3 2 4	2.040	31
4.261	38	4 0 0	4.255	35	1 1 1	4.704	13	1 9 4 7	39	7 2 1	1.947	40	3 2 2	1.947	43	
3.945	4		3.939	12	2 0 0	4.258	67	1 8 6 0	4	3 2 3	1.860	9	1 2 6	1.861	4	
3.930	3.927							0 0 3	3.946	11	1.838	18	0 4 0	1.839	25	
								0 1 3	3.922	10	1.823	14	9 0 1	1.824	8	
								0 1 3	3.918	30	1.777	2	2 4 0	1.797	1	
								2 1 1	3.893	2	1.752	10	7 2 2	1.752	14	
														0 0 8	1.753	13
														1 0 8	1.715	17
														2 0 8	1.715	8
														5 2 6	1.711	19
														10 0 0	1.703	4
														9 2 0	1.683	8
														4 2 0	1.683	9
														5 0 2	1.653	13
														10 0 2	1.653	4
														9 2 2	1.639	3
														4 4 1	1.640	9
														4 2 2	1.639	6
														2 4 2	1.600	10
														2 4 4	1.602	14
														2 4 4	1.602	8
														4 0 6	1.579	10
														8 0 6	1.579	4
														9 2 4	1.521	12
														6 0 2	1.393	17
														12 0 2	1.393	6
														5 2 6	1.369	1
														9 2 6	1.369	3
														8 0 8	1.357	5
														8 0 8	1.357	2
														8 0 8	1.349	2
														10 1 3	1.349	3
														4 0 8	1.349	6
														8 0 8	1.349	2

b: broad. Values of *d* are expressed in Å.

fraction File), which was later replaced by PDF 23–0125 pertaining to hydrothermally synthesized xonotlite. Nevertheless, peak intensities are not comparable because of preferred orientations caused by the perfect {*h0l*} cleavage of xonotlite; in particular, the reflections at 3.247 and 2.697 Å are greatly enhanced. The PDF 72–2396 card is a calculated pattern of a natural specimen from South Osettia, Russia, on the basis of the monoclinic polytype of xonotlite of Mamedov & Belov (1955). This later diffraction pattern differs significantly from the spacings of the PDF 29–0379 (specimen from Huntly, Scotland), taking into account the differences of the reported unit-cell parameters.

Crystals of xonotlite, as of many other calcium silicate hydrates, represent polytypic intergrowths with additional twinning and disorder (Merlino *et al.* 2000, Hejny & Armbruster 2001). In nature, five polytypes of xonotlite have been identified: three are ordered and two are one-dimensionally disordered (Gard 1966), the most widespread being the *Ma2b2c* polytype, followed by the *Ma2bc* polytype (Chisholm 1980). However, recent investigations have shown the predominance of the *M2a2b2c* polytype in some locations (Kudoh &

Takéuchi 1979, Hejny & Armbruster 2001). Owing to the absence of published diffraction-patterns of all the polytypes of xonotlite, we compared our data (*d*_{obs}) with calculated XRPD patterns (*d*_{calc} in Table 2) for the ordered polytypes, following the data of Hejny & Armbruster (their Tables 1 to 5) and using the CRYSTALDIFFRACT software package (Palmer 1999).

Comparisons of the recorded XRPD pattern with the calculated diffraction-patterns allow us to discard *M2a2b2c* (not yet found in nature) and *Ma2bc* and select *M2a2b2c* and *Ma2b2c* polytypes as the most probable in the samples from the Ronda Peridotites. The calculated diffraction-patterns of xonotlite *M2a2b2c* and *Ma2b2c* are very similar in the 25–70° 2θ range, but the *M2a2b2c* polytype can be distinguished by the presence of lines at 6.400, 5.645, 4.704, 3.918 and 3.721 Å, whereas the *Ma2b2c* polytype displays weaker peaks at 6.519, 6.082, 5.169, 3.840 and 3.573 Å. In the recorded pattern, some of these reflections could not clearly be identified owing to preferred orientation. The presence of some very weak, asymmetrical and broad peaks with intensity maxima at 6.499, 3.933 and 2.637 Å define

well the presence of these two common polytypes in the xonotlite samples from the Ronda Peridotites. These broad peaks were fit with the Pearson VII function to perform the deconvolution of overlapping peaks by the use of a freeware software package (MacDiff 4.2.4a; Petschick 2001). In this way, the lines at 6.418, 3.927 and 3.901 Å were used to identify xonotlite *M2a2b2c*, and lines at 6.505, 6.077, 3.945 and 2.596, to identify xonotlite *Ma2b2c*. Some other low-intensity peaks also aided in the identification of polytypes, *i.e.*, peaks at 2.167 and 2.129 Å for *M2a2b2c* polytype, and at 3.845 and 2.105 Å for xonotlite *Ma2b2c*.

Pattern PDF 29–0379 pertains to a mixture of the *M2a2b2c* and *Ma2b2c* polytypes and gives a better fit with our pattern (Table 2) than other diffraction patterns included in the JCPDS File (*i.e.*, PDF 23–0125 and 72–2396).

DISCUSSION

In this work, we report the occurrence of xonotlite in the Ronda peridotites. We have documented the widespread rodingitization of granitic dykes that intruded the Carratraca massif, close to the Cerro Tajo fault. This finding raises a number of issues, such as the relationships between the Cerro Tajo fault, and the serpentinization and the late stages of emplacement of the Ronda peridotites, at low-pressure and low-temperature conditions. As an additional implication of our finding for the tectonic evolution of the Betic Cordilleras, the presence of rodingites can no longer be considered a petrogenetic feature to distinguish between the ultramafic suite of the Nevado–Filábride complex and the Ronda peridotites, as claimed by Puga *et al.* (1999). These authors commented on the absence of rodingite in the Ronda peridotites, which contrasts with the evidence shown in this paper. However, there are relevant differences in the timing and geological setting of both rodingite associations. Rodingites from the Ronda peridotites were produced in Miocene times, during the extensional collapse of the Betic Cordilleras. In contrast, according to Puga *et al.* (1999), the Nevado–Filábride rodingites developed close to an oceanic spreading center during Upper Jurassic times.

The Cerro Tajo outcrop provides the following constraints for the low-pressure emplacement of the Ronda peridotites: 1) Intrusion of granitic dykes into the Ronda peridotites took place at high-temperature and low-pressure conditions (725°C, 350 MPa) (Westerhof 1975). This estimate is based on the widespread presence of cordierite, produced by the partial melting of the metamorphic sequences underlying the Ronda peridotites during emplacement. The time of intrusion of the dykes is constrained by a Rb/Sr age of 22.2 ± 4 Ma, obtained from a small intrusion of cordierite-bearing granite into the peridotite of the Sierra Bermeja (Priem *et al.* 1979). 2) Subsequent events developed at decreasing temperature, below 500°C, leading to the serpentinization of the

ultramafic rocks. 3) The final episode is represented by the rodingitization of the leucocratic dykes at a temperature below 350°C (Buckner *et al.* 1960, O'Brien & Rodgers 1973, Honnorez & Kirst 1975).

The extent of the serpentinization decreases with increasing distance from the Cerro Tajo fault. The shear zone thus favored the percolation of fluids that produced the serpentinization of the ultramafic rocks. Also, pressure must have dropped to below 200 MPa during the serpentinization, as higher confining pressure prevents the existence of open cracks (Paterson 1978). Therefore, we propose that at Cerro Tajo, the serpentinization was largely induced by surface water percolating down the shear zone. An external origin for the serpentinizing fluids has been proposed by Acosta-Vigil *et al.* (2001), to account for the high content of boron in serpentinites at the contact between granitic dykes and peridotites from Sierra Bermeja.

Rodingites are formed through Ca enrichment and silica loss in the rocks adjacent to or within serpentinized peridotites (O'Hanley 1996). Schandl *et al.* (1989) established a correlation between the degree of rodingite formation and the assemblages of serpentine minerals in a serpentinite and adjacent rodingite: lizardite in the serpentinite with epidote-group minerals in the rodingite, chrysotile with grossular, and antigorite with diopside, progressing from the earlier stage of alteration to the most advanced stage. The features observed in Cerro Tajo: prehnite – hydrogrossular – xonotlite association, loss of silica in the dykes and the formation of albite in association to pectolite, can be explained by rodingitization processes during the serpentinization of the Ronda orogenic peridotites. The formation of this unusual rodingitic association seems to require several episodes of metasomatic interaction between the granitic dykes and the host ultrabasic rocks. A first percolation of Ca-enriched fluids could have led to the initial development of hydrogrossular, pectolite and prehnite. The replacement of hydrogrossular by xonotlite points to a second metasomatic event, and the existence of fracture-filling pectolite or xonotlite suggests equilibration with late fluids. The chlorite selvage probably represents localized Mg-metasomatism of the granitic dyke, rather than metasomatized serpentinite, as proposed by Wares & Martin (1980) for a rodingitized felsic dyke in the Jeffrey mine, in Quebec. Some near-surface alteration has occurred since then, producing, aragonite along joint surfaces, for example.

The amount of xonotlite increases with increased rodingitization: during incipient stages of rodingitization, xonotlite is dispersed throughout the reaction zone, but in the final stages, xonotlite forms continuous veins that may pervade the dyke and the nearby serpentinite. The association of xonotlite with hydrogrossular, in the presence of pectolite, prehnite and albite, points to a temperature range between 275 to 400°C (Buckner *et al.* 1960), more probably between 300 and 350°C (Fyfe & Turner 1958, Karup-Møller 1969), in line with the

existence of lizardite in the surrounding serpentinites. Available data are not sufficient to identify the precursor mineral of xonotlite.

The xonotlite from the Ronda peridotites exhibits a morphology, chemical composition and X-ray powder-diffraction patterns similar to xonotlite reported in the literature. There are slight chemical differences among xonotlite samples associated with hydrogrossular, and no significant differences were found between acicular and tabular xonotlite.

ACKNOWLEDGEMENTS

We are grateful to Drs. M. Obata, F.J. Wicks and R.F. Martin for their constructive comments, which helped to improve the paper. Financial support from the projects PB96-1452-CO3-03, BTE2001-0634, UPV0001.310-14478/2002 and GI18/99 is acknowledged. DTA/TGA analyses were carried out by A. Aguayo at the "Laboratorio de Ingeniería Química" of the Universidad del País Vasco. We are also grateful to J.A. Ibañez for running XRD analyses of xonotlite and J. Arostegui, J.M. Herrero, P.P. Gil and J.L. Pizarro (Dpto. de Mineralogía y Petrología, Universidad del País Vasco) for help with diffractometric studies.

REFERENCES

- ACOSTA-VIGIL, A., PEREIRA, M.D., SHAW, D.M. & LONDON, D. (2001): Contrasting behaviour of boron during crustal anatexis. *Lithos* **56**, 15-31.
- ARGLES, T.W., PLATT, J.P. & WATERS, D.J. (1999): Attenuation and excision of a crustal section during extensional exhumation: the Carratraca Massif, Betic Cordillera, southern Spain. *J. Geol. Soc. London* **156**, 149-162.
- BAUER, L.H. & BERMAN, H. (1935): Xonotlite from Franklin Furnace. *Am. Mineral.* **20**, 197.
- BROWN, P.A. (1978): Xonotlite: a new occurrence at Rose Blanche, Newfoundland. *Can. Mineral.* **16**, 671-672.
- BUCKNER, D. A., ROY, D. M. & ROY, R. (1960): Studies in the system CaO-Al₂O₃-SiO₂-H₂O, II. The system CaSiO₃-H₂O. *Am. J. Sci.* **258**, 132-147.
- CHISHOLM, J.E. (1980): Polytypism in xonotlite, Ca₆Si₆O₁₇(OH)₂. In *Electron Microscopy and Analysis, 1979. Inst. Phys. Conf. Ser.* **52**, 109-112.
- COLEMAN, R.G. (1967): Low temperature reaction zones and alpine ultramafic rocks of California, Oregon, and Washington. *U.S. Geol. Surv., Bull.* **1247**, 1-49.
- COOMBS, D.S. & LAUDER, W.R. (1960): Note on xonotlite from Acheron River, mid-Canterbury. *N.Z. J. Geol. Geophys.* **3**, 72-73.
- COULTON, A.J., HARPPER, G.D. & O'HANLEY, D.S. (1995): Oceanic versus emplacement age serpentinization in the Josephine ophiolite: implications for the nature of the Moho at intermediate and slow spreading ridges. *J. Geophys. Res.* **100**, 22,245-22,260.
- DE BRUIJN, H., SCHOCH, A.E., VAN DER WESTHUIZEN, W.A. & BEUKES, G.J. (1999): The chemical composition of xonotlite and associated inesite from the Nchwaning and Wessels mines, Kalahari manganese field, South Africa. *Neues Jahrb. Mineral., Monatsh.*, 212-222.
- DEWEY, J.F., HELMAN, M.L., TURCO, E., HUTTON, D.E.H. & KNOTT, S.D. (1989): Kinematics of the western Mediterranean. In *Alpine Tectonics* (M.P. Coward, D. Dietrich & R.G. Park, eds.). *Geol. Soc., Spec. Publ.* **45**, 265-283.
- DICKEY, J.S., JR. & OBATA, M. (1974): Graphitic hornfels dikes in the Ronda high-temperature peridotite massif. *Am. Mineral.* **59**, 1183-1189.
- FYFE, W.S. & TURNER, F.J. (1958): Correlation of metamorphic facies with experimental data. In *Metamorphic Reactions and Metamorphic Facies* (W.S. Fyfe, F.J. Turner & J. Verhoogen, eds.). *Geol. Soc. Am., Mem.* **73**, 149-185.
- GARD, J.A. (1966): A system of nomenclature for the fibrous calcium silicates, and a study of xonotlite polytypes. *Nature* **211**, 1078-1079.
- HARKER, R.I. (1964) : Dehydration series in the system CaSiO₃-SiO₂-H₂O. *J. Am. Ceram. Soc.* **47**, 521-529.
- HEJNY, C. & ARMBRUSTER, T. (2001): Polytypism in xonotlite Ca₆Si₆O₁₇(OH)₂. *Z. Kristallogr.* **216**, 396-408.
- HERNÁNDEZ-PACHECO, A. (1968): Estudio petrográfico y geoquímico del macizo ultramáfico de Ojén (Málaga). *Estudios Geol.* **23**, 85-143.
- HONNOREZ, J. & KIRST, P. (1975): Petrology of rodingites from the equatorial mid-Atlantic fracture zones and their geotectonic significance. *Contrib. Mineral. Petrol.* **40**, 233-257.
- JAKOBSSON, S.P. & MOORE, J.G. (1986): Hydrothermal minerals and alteration rates at Surtsey Volcano, Iceland. *Geol. Soc. Am., Bull.* **97**, 648-659.
- KARUP-MØLLER, S. (1969): Xonotlite-, pectolite- and natrolite-bearing fracture veins in volcanic rocks from Nûgssuaq, West Greenland. *Meddel. om Gronland* **186**, 1-20.
- KAYE, C.A. (1953) : A xonotlite occurrence in Puerto Rico. *Am. Mineral.* **38**, 860-862.
- KUDOH, Y. & TAKÉUCHI, Y. (1979): Polytypism of xonotlite. I. Structure of an $\bar{A}1$ polytype. *Mineral. J.* **9**, 349-373.
- LUNDEEN, M.T. (1978): Emplacement of the Ronda peridotite, Sierra Bermeja, Spain. *Geol. Soc. Am., Bull.* **89**, 172-180.
- LUQUE, F.J., RODAS, M. & GALÁN, E. (1992): Graphite vein mineralization in the ultramafic rocks of southern Spain: mineralogy and genetic relationships. *Mineral. Deposita* **27**, 226-233.

- _____, _____, VELASCO, F. & GALÁN, E. (1987): Mineralogía y geotermometría de los diques ácidos con grafito asociados a rocas ultramáficas de la Serranía de Ronda, Málaga. *Estudios geol.* **43**, 367-375.
- MAMEDOV, K.S. & BELOV, N.V. (1955): Crystal structure of xonotlite. *Dokl. Akad. Nauk SSSR* **104**, 615-618 (in Russ.).
- MERLINO, S., BONACCORSI, E. & ARMBRUSTER, T. (2000): The real structures of clinotobermorite and tobermorite 9Å: OD character, polytypes, and structural relationships. *Eur. J. Mineral.* **12**, 411-426.
- NAVARRO-VILÁ, F. & TUBÍA, J.M. (1983): Essai d'une nouvelle différenciation des Nappes Alpujarrides dans le secteur occidental des Cordillères Bétiques (Andalousie, Espagne). *C.R. Acad. Sci. Paris* **296**, 111-114.
- OBATA, M. (1980): The Ronda peridotite: garnet-, spinel-, and plagioclase-lherzolite facies and the P-T trajectories of a high temperature mantle intrusion. *J. Petrol.* **21**, 533-572.
- O'BRIEN, J.P. & RODGERS, K.A. (1973): Xonotlite and rodingites from Wairere, New Zealand. *Mineral. Mag.* **39**, 233-240.
- O'HANLEY, D.S. (1996): *Serpentinities. Records of Tectonic and Petrological History*. Oxford University Press, New York, N.Y.
- PALMER, D.C. (1999): *CrystalDiffract, Powder Diffraction Software*. CrystalMaker Software, Oxfordshire, U.K.
- PATERSON, M.S. (1978): *Experimental Rock Deformation. The Brittle Field*, Springer-Verlag, Berlin, Germany.
- PETSCHICK, R. (2001): MacDiff 4.2.4a, Powder diffraction Software. Manual. <http://servermac.geologi.uni-frankfurt.de/Rainer.html>. Johann Wolfgang Goethe-Univ. Frankfurt am Main, Germany.
- PRIEM, H.N.A., BOELRIJK, N.A.I.M., HEBEDA, E.H., OEN, I.S., VERDURMEN, E.A.T. & VERSCHURE, R.H. (1979): Isotopic dating of the emplacement of the ultramafic masses in the Serrania de Ronda, southern Spain. *Contrib. Mineral. Petrol.* **70**, 103-109.
- PUGA, E., NIETO, J.M., DÍAZ DE FEDERICO, A., BODINIER, J.L. & MORTEN, L. (1999): Petrology and metamorphic evolution of ultramafic rocks and dolerite dykes of the Betic Ophiolitic Association (Mulhacén Complex, SE Spain): evidence of eo-Alpine subduction following an ocean-floor metasomatic process. *Lithos* **49**, 23-56.
- RAMMELSBERG, C. (1866): Über den Xonaltit, ein neues wasserhaltiges Kalksilikat, und den Bustamit aus Mexiko. *Z. deutsch. geol. Ges.* **18**, 33-34.
- ROY, D.M. (1958): Studies in the system CaO-Al₂O₃-SiO₂-H₂O. IV. Phase equilibria in the high-lime portion of the system CaO-SiO₂-H₂O. *Am. Mineral.* **43**, 1009-1029.
- SCHANDL, E.S., O'HANLEY, D.S. & WICKS, F.J. (1989): Rodingites in serpentinized ultramafic rocks of the Abitibi greenstone belt, Ontario. *Can. Mineral.* **27**, 579-591.
- _____, _____ & KYSER, T.K. (1990): Fluid inclusions in rodingite: a geothermometer for serpentinization. *Econ. Geol.* **85**, 1273-1276.
- SCHWARTZ, G.M. (1924): An occurrence of xonotlite in Minnesota. *Am. Mineral.* **9**, 32-33.
- _____. (1925): Xonotlite and pectolite in a diabase pegmatite from Minnesota. *Am. Mineral.* **10**, 83-88.
- SHANNON, E.V. (1925): An occurrence of xonotlite at Leesburg, Virginia. *Am. Mineral.* **10**, 12-13.
- SHAW, S., HENDERSON, C.M.B. & KOMANSCHER, B.U. (2000): Dehydration/recrystallization mechanisms, energetics, and kinetics of hydrated calcium silicate minerals: an in situ TGA/DSC and synchrotron radiation SAXS/WAXS study. *Chem. Geol.* **167**, 141-159.
- SMITH, C.H. (1954): On the occurrence and origin of xonotlite. *Am. Mineral.* **39**, 531-532.
- SPEAKMAN, K. (1968): The stability of tobermorite in the system CaO-SiO₂-H₂O at elevated temperatures and pressures. *Mineral. Mag.* **36**, 1090-1103.
- TAYLOR, H.F.W. (1959): The transformation of tobermorite into xonotlite. *Mineral. Mag.* **32**, 110-116.
- TUBÍA, J.M. (1994): The Ronda peridotites (Los Reales nappe): an example of the relationship between lithospheric thickening by oblique tectonics and late extensional deformation within the Betic Cordillera (Spain). *Tectonophysics* **238**, 381-398.
- _____. & CUEVAS, J. (1986): High-temperature emplacement of the Los Reales peridotite nappe (Betic Cordillera, Spain). *J. Struct. Geol.* **8**, 473-482.
- _____, _____, NAVARRO-VILÁ, F., ÁLVAREZ, F. & ALDAYA, F. (1992): Tectonic evolution of the Alpujarride Complex (Betic Cordillera, southern Spain). *J. Struct. Geol.* **14**, 193-203.
- VAN DER WAL, D. & VISSERS, L.M. (1996): Structural petrology of the Ronda peridotite, SW Spain: deformation history. *J. Petrol.* **37**, 23-43.
- WARES, R.P. & MARTIN, R.F. (1980): Rodingitization of granite and serpentinite in the Jeffrey mine, Asbestos, Quebec. *Can. Mineral.* **18**, 231-240.
- WESTERHOF, A.B. (1975): *Genesis of Magnetite Ore near Marbella, Southern Spain: Formation by Oxidation of Silicates in Polymetamorphic Gedrite-Bearing and other Rocks*. Ph.D. thesis, Univ. of Amsterdam, The Netherlands. GUA Papers in Geology.